

**An experimental and theoretical study of exciplex-forming compounds containing  
trifluorobiphenyl and 3,6-di-*tert*-butylcarbazole units and their performances in OLEDs**

**R. Keruckiene<sup>1</sup>, M. Guzauskas<sup>1</sup>, L. Lapienyte<sup>1</sup>, J. Simokaitiene<sup>1</sup>, D. Volyniuk<sup>1</sup>, J. Cameron<sup>2</sup>, P.  
J. Skabara<sup>2</sup>, G. Sini<sup>3</sup> and J. V. Grazulevicius<sup>1\*</sup>**

*<sup>1</sup>Department of Polymer Chemistry and Technology, Kaunas University of Technology, K. Barsausko  
St. 59, LT-50254, Kaunas, Lithuania*

*<sup>2</sup>WestCHEM, School of Chemistry, University of Glasgow, Joseph Black Building, University Place,  
Glasgow, G12 8QQ, UK*

*<sup>3</sup>Laboratoire de Physicochimie des Polymères et des Interfaces, CY Paris Seine Université, EA 2528,  
5 mail Gay-Lussac, Cergy-Pontoise Cedex 95031, France*

---

\*Corresponding authors: Juozas Vidas Grazulevicius. E-mail address: juozas.grazulevicius@ktu.lt; Gjergji Sini. E-mail address: gjergji.sini@u-cergy.fr; Peter Skabara. E-mail address: Peter.Skabara@glasgow.ac.uk

## Table of Contents

|  |    |
|--|----|
| <b>Experimental</b> .....  | 3  |
| <b>Table S1.</b> Summary of singlet excitations for TDDFT calculations of <b>1</b> and <b>2</b> with default $\omega$ or $\omega$ -CPCM.....                       | 8  |
| <b>Figure S1.</b> DSC and TGA thermograms of compounds <b>1</b> and <b>2</b> .....   | 9  |
| <b>Figure S2.</b> Cyclic voltammograms of solid samples of compounds <b>1</b> and <b>2</b> . ....  | 10 |
| <b>Figure S3.</b> Absorption and fluorescence spectra of 9H-carbazole toluene solution.....  | 10 |
| <b>Figure S4.</b> Transitions for $T_1$ excitation of compound <b>1</b> determined by TDDFT. $\omega$ B97XD/6-31++G(d,p), default $\omega$ .....                   | 11 |
| <b>Figure S5.</b> Transitions for $S_1$ excitation of compound <b>1</b> determined by TDDFT. $\omega$ B97XD/6-31++G(d,p), default $\omega$ .....                   | 12 |
| <b>Figure S6.</b> Transitions for $T_1$ excitation of compound <b>1</b> determined by TDDFT. $\omega$ B97XD/6-31++G(d,p), $\omega$ -CPCM.....                      | 13 |
| <b>Figure S7.</b> Transitions for $S_1$ excitation of compound <b>1</b> determined by TDDFT. $\omega$ B97XD/6-31++G(d,p), $\omega$ -CPCM.....                      | 14 |
| <b>Figure S8.</b> Transitions for $T_1$ excitation of compound <b>2</b> determined by TDDFT. $\omega$ B97XD/6-31++G(d,p), default $\omega$ .....                   | 16 |
| <b>Figure S9.</b> Transitions for $S_1$ excitation of compound <b>2</b> determined by TDDFT. $\omega$ B97XD/6-31++G(d,p), default $\omega$ .....                   | 16 |
| <b>Figure S10.</b> Transitions for $T_1$ excitation of compound <b>2</b> determined by TDDFT. $\omega$ B97XD/6-31++G(d,p), $\omega$ -CPCM.....                     | 17 |
| <b>Figure S11.</b> Transitions for $S_1$ excitation of compound <b>2</b> determined by TDDFT. $\omega$ B97XD/6-31++G(d,p), $\omega$ -CPCM.....                     | 18 |
| <b>Figure S12.</b> Fluorescence spectra of solid films of carbazole-substituted compounds <b>1</b> and <b>2</b> .....  | 10 |
| <b>Figure S13.</b> Fluorescence intensity dependence on laser pump pulse energy of solid samples of compound <b>1</b> and <b>2</b> at RT with delay of 800 ns..... | 10 |

## Experimental

### Instrumentation

**Nuclear magnetic resonance (NMR) spectroscopy.**  $^1\text{H}$  spectra were recorded by a *Bruker Avance III* apparatus (400 MHz). The samples were prepared by dissolving ca. 20 mg of a compound in 1 ml of deuterated chloroform ( $\text{CDCl}_3$ ). Hydrogen nuclei  $^1\text{H}$  were excited using the frequency of 400 MHz. The data are presented as chemical shifts ( $\delta$ ) in ppm (in parentheses: multiplicity, integration, coupling constant).

**Attenuated total reflectance infrared spectroscopy (ATR-IR).** IR spectra were recorded by using a *Vertex 70 Bruker* spectrometer equipped with an ATR attachment with a diamond crystal over frequencies of  $600\text{--}3500\text{ cm}^{-1}$  with a resolution of  $5\text{ cm}^{-1}$  over 32 scans. IR spectra are presented as a function of transparency (T) expressed in percent (%) against the wavenumber ( $\nu$ ) expressed in  $\text{cm}^{-1}$ .

**Mass spectrometry.** Mass spectra were obtained on a *Waters ZQ 2000* mass spectrometer.

**Melting points** of the compounds were determined by using an Electrothermal MEL-TEMP apparatus.

**UV-VIS absorption spectroscopy.** Absorption spectra of the dilute solutions ( $10^{-4}\text{--}10^{-5}\text{ mol/l}$ ) and thin films of the compounds were recorded under ambient conditions with a *Perkin Elmer Lambda 25* spectrophotometer.

**Photoluminescence (PL) spectroscopy.** Fluorescence spectra of thin films and dilute solutions ( $10^{-4}\text{--}10^{-5}\text{ mol/l}$ ) of the compounds were recorded at room temperature with a luminescence spectrometer *Edinburgh Instruments FLS980*. PL quantum yields of the solutions and thin films were measured using an integrating sphere. Phosphorescence spectra were recorded at 77 K.

**Differential scanning calorimetry (DSC)** measurements were carried out using a *TA Instruments Q2000* thermosystem. The samples were examined at a heating/cooling rate of 10 °C/min under nitrogen atmosphere.

**Thermogravimetric analysis (TGA)** was performed under nitrogen atmosphere on a *TA Instruments Q50* analyser. The heating rate was 20 °C/min.

**Photoelectron emission spectrometry** was used to determine the ionisation energies (IE) of the layers of the synthesised compounds <sup>1</sup>. For the recording of the photoelectron emission spectra, the layers were prepared by drop-casting chloroform solutions of the materials onto cleaned indium tin oxide (ITO)-coated glass substrates. A negative voltage of 300 V was applied to the sample substrate. A deep UV deuterium light source ASBN-D130-CM and CM110 1/8 m monochromator were used for the illumination of the samples with monochromatic light. A *6517B Keithley* electrometer was connected to the counter-electrode for the measurement of the photocurrent which was flowing in the circuit under illumination. An energy scan of the incident photons was performed while increasing the photon energy. The photocurrent (which is attributed to  $dU/dt$ ) is dependent on the incident light photon energy ( $h\nu$ ). The IE was estimated as the intersection points of the extrapolated linear part of the dependence  $(dU/dt)^{1/2}=f(h\nu)$  and the  $h\nu$  axis (i.e. the  $h\nu$  value at zero photocurrent).

**Cyclic voltammetry** measurements were performed by using a glassy carbon working electrode (a disk with the diameter of 2 mm) in a three-electrode cell of Autolab Type potentiostat – galvanostat. The measurements were carried out for the solutions in dry dichloromethane containing 0.1 M tetrabutylammonium hexafluorophosphate at 25 °C; the scan rate was 50 mV/s while the sample concentration was  $10^{-3}$  M. The potentials were measured against silver as a quasi-reference electrode. Platinum wire was used as a counter electrode. The potentials were calibrated with the standard ferrocene/ferrocenium (Fc/Fc<sup>+</sup>) redox system <sup>2</sup>.

**Computational methods.** All calculations were carried out in the frame of density functional theory (DFT) by using  $\omega$ B97XD functional<sup>3</sup> in conjunction with the 6-31++G(d,p) basis set: (i) Firstly, the geometry optimisation, and the study of the electronic structure and optical properties of both molecules were carried out by using the default value for the  $\omega$  parameter (0.2 bohr<sup>-1</sup>). The impact of the environment at this step was considered by simply using conductor-like polarisable continuum model (CPCM)<sup>4</sup> for solvation with diethyl ether ( $\epsilon = 4.12$ ). (ii) In a second step, the value for the  $\omega$  parameter was tuned<sup>5</sup> by considering the impact of diethyl ether, resulting in a much smaller  $\omega$  (0.011 bohr<sup>-1</sup>) as compared to the default one. The tuned  $\omega$  parameter will be reported hereafter as  $\omega$ -CPCM. The geometries of both molecules were optimised subsequently by using  $\omega$ -CPCM = 0.011 bohr<sup>-1</sup>. This last geometry (reported hereafter as geom-solvent) was used subsequently for each molecule during time-dependent density functional theory (TDDFT) calculations, in which the impact of the solvent was additionally included by using  $\omega$ -CPCM = 0.011 bohr<sup>-1</sup>. As such, the impact of the solvent was introduced by using geom-solvent in conjunction with  $\omega$ -CPCM, without utilising the CPCM method further.

In order to quantify the degree of CT for the calculated excitations, the spatial overlap ( $\Lambda$ ) for linear excitations from TDDFT was calculated using a method described by Tozer *et al.*<sup>6</sup> where each contribution ( $\kappa$ ) is scaled (equations 1 and 2).

$$\Lambda = \frac{\sum_{i,a} \kappa_{ia}^2 O_{ia}}{\sum_{i,a} \kappa_{ia}^2} \quad (1)$$

$$O_{ia} = \int |\varphi_i(r)| |\varphi_a(r)| dr \quad (2)$$

All calculations were carried out using Gaussian 09 rev D.01 software.<sup>7</sup>

## Materials

1-Bromo-3-iodobenzene, 1-bromo-3,5-difluorobenzene (purchased from TCI Europe), 9H-carbazole, cesium carbonate, copper, 18-crown-6, palladium (0) tetrakis(triphenylphosphine), potassium hydroxide, 2,4,6-trifluorophenylboronic acid, *tert*-butylchloride, zinc chloride (purchased from Aldrich), were used as received. Thin layer chromatography was performed by using TLC plates covered with a silica gel matrix on aluminium backing (purchased from Aldrich). 3,6-Di-*tert*-butylcarbazole was synthesised according to the reported procedure <sup>8</sup>. 9-(3-Bromophenyl)-3,6-di-*tert*-butylcarbazole (**BrPhmCz**) was synthesised according to reference <sup>9</sup>. 9,9'-(5-Brom-1,3-phenylene)bis(3,6-di-*tert*-butylcarbazole) (**BrPhdiCz**) was synthesised according to a previously reported literature procedure <sup>10</sup>.

Target compounds **1–2** were synthesised by employing Suzuki coupling reaction <sup>11</sup>. A mixture of brominated intermediate compounds **BrPhmCz** or **BrPhdiCz**, 2,4,6-trifluorophenylboronic acid, and cesium carbonate was placed under vacuum into a Schlenk flask and then backfilled with nitrogen three times before adding N,N-dimethylformamide. The reaction mixture was refluxed overnight. After cooling to ambient temperature, it was poured into water. The aqueous phase was extracted with CH<sub>2</sub>Cl<sub>2</sub> (3 × 50 ml); the combined organic phases were dried over sodium sulfate, filtered, and then the solvent was removed. The target product was purified by column chromatography on silica using hexane as eluent.

### 9-(2,4,6-Trifluoro-[1,1'-biphenyl]-3'-yl)-3,6-di-*tert*-butylcarbazole (**1**)

Intermediate compound **BrPhmCz** (0.55 g, 1.2 mmol), 2,4,6-trifluorophenylboronic acid (0.28 g, 1.6 mmol) and cesium carbonate (0.81 g, 2.5 mmol) in DMF (15 ml) were used for the synthesis of compound **1**. The yield of white crystals was 37% (0.213 g). T<sub>M</sub>=134 °C (DSC). C<sub>32</sub>H<sub>30</sub>F<sub>3</sub>N. <sup>1</sup>H NMR (400 MHz, CDCl<sub>3</sub>) δ 8.06 (d, *J* = 5.0 Hz, 2H), 7.66 (s, 2H), 7.60 – 7.32 (m, 6H), 7.27 (d, *J* = 8.6 Hz, 2H), 1.39 (s, 18H). <sup>13</sup>C NMR (101 MHz, CDCl<sub>3</sub>) δ 143, 142, 139, 138, 131, 130, 129, 126, 124, 123,

116, 109, 77, 76, 34, 32, 30. ATR-IR (solid state on ATR, cm<sup>-1</sup>): 3057 (Ar. C–H), 2953, 2926 (Alk. C–H), 1361(Alk. C–N),1294, 1260, (Alk. C–F). MW=485.17 g/mol. MS(APCI<sup>+</sup>, 20 V), m/z=486 [(M+H)<sup>+</sup>].

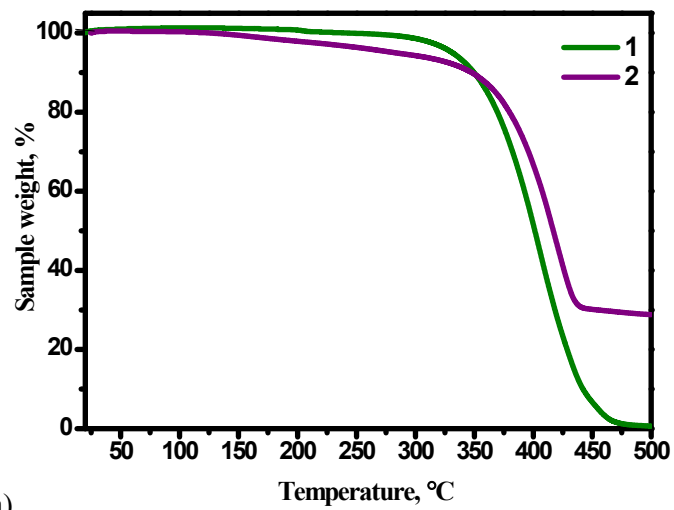
**9,9'-(2,4,6-Trifluoro-[1,1'-biphenyl]-3',5'-yl)bis(3,6-di-*tert*-butylcarbazole) (2)**

Intermediate compound **BrPhdiCz** (0.35 g, 0.493 mmol), 2,4,6-trifluorophenylboronic acid (0.32 g, 1.87 mmol) and cesium carbonate (0.81 g, 2.5 mmol) in DMF (15 ml) were used for the synthesis of compound **2**. The yield of white crystals was 39% (0.132g). T<sub>M</sub>=292 °C (DSC). C<sub>52</sub>H<sub>53</sub>F<sub>3</sub>N<sub>2</sub>. <sup>1</sup>H NMR (400 MHz, CDCl<sub>3</sub>) δ 8.05 (d, *J* = 17.8 Hz, 4H), 7.83 – 7.63 (m, 2H), 7.56 (d, *J* = 7.8 Hz, 2H), 7.50 – 7.30 (m, 8H), 6.76 (t, *J* = 8.2 Hz, 1H), 1.38 (d, *J* = 6.4 Hz, 36H). <sup>13</sup>C NMR (101 MHz, CDCl<sub>3</sub>) δ 143, 142, 138, 137, 129, 124, 123, 122, 116, 115, 109, 108, 76, 75, 33, 30. ATR-IR (solid state on ATR, cm<sup>-1</sup>): 3057 (Ar. C–H), 2953, 2926 (Alk. C–H), 1361(Alk. C–N),1294, 1260, (Alk. C–F). MW=762.42 g/mol, MS (APCI<sup>+</sup>, 20 V), m/z=763 [(M+H)<sup>+</sup>].

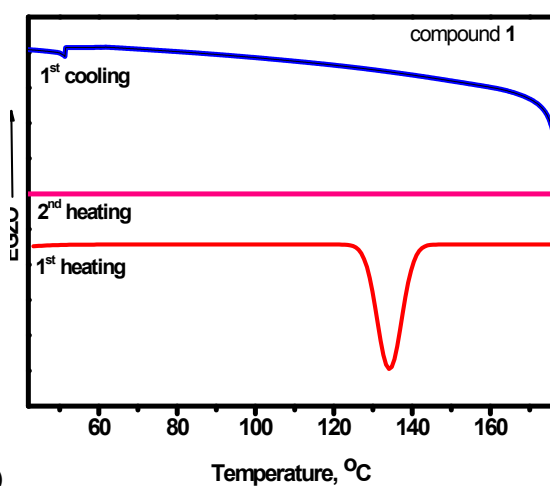
**Table S1.** Summary of singlet excitations for TDDFT calculations of **1** and **2** with default  $\omega$  or  $\omega$ -CPCM

| Compound | Method           | Excitation      | $\lambda$ (nm) | f      | Dominant transition          | Transition description <sup>a</sup> |
|----------|------------------|-----------------|----------------|--------|------------------------------|-------------------------------------|
| <b>1</b> | Default $\omega$ | S <sub>1</sub>  | 294.7          | 0.10   | HOMO $\rightarrow$ LUMO+1    | LE                                  |
|          |                  | S <sub>2</sub>  | 265.4          | 0.20   | HOMO $\rightarrow$ LUMO      | LE + CT                             |
|          |                  | S <sub>3</sub>  | 263.7          | 0.45   | HOMO-1 $\rightarrow$ LUMO+1  | LE + CT                             |
|          |                  | S <sub>4</sub>  | 258.6          | 0.49   | HOMO $\rightarrow$ LUMO+2    | LE + CT                             |
|          |                  | S <sub>5</sub>  | 241.6          | 0.53   | HOMO $\rightarrow$ LUMO+10   | LE + CT                             |
|          |                  | S <sub>6</sub>  | 230.2          | 0.01   | HOMO-5 $\rightarrow$ LUMO    | LE                                  |
|          |                  | S <sub>7</sub>  | 226.4          | 0.09   | HOMO $\rightarrow$ LUMO+3    | LE+CT                               |
|          |                  | S <sub>8</sub>  | 225.5          | 0.66   | HOMO-2 $\rightarrow$ LUMO    | LE+CT                               |
|          |                  | S <sub>9</sub>  | 222.5          | 0.80   | HOMO-3 $\rightarrow$ LUMO+1  | LE+CT                               |
|          |                  | S <sub>10</sub> | 218.9          | 0.46   | HOMO-1 $\rightarrow$ LUMO+11 | LE+CT                               |
| <b>1</b> | $\omega$ -CPCM   | S <sub>1</sub>  | 325.1          | 0.01   | HOMO $\rightarrow$ LUMO      | CT                                  |
|          |                  | S <sub>2</sub>  | 313.2          | 0.003  | HOMO $\rightarrow$ LUMO+1    | LE + CT                             |
|          |                  | S <sub>3</sub>  | 312.5          | 0.04   | HOMO $\rightarrow$ LUMO+3    | LE                                  |
|          |                  | S <sub>4</sub>  | 293.0          | 0.007  | HOMO $\rightarrow$ LUMO+2    | CT                                  |
|          |                  | S <sub>5</sub>  | 289.7          | 0.001  | HOMO $\rightarrow$ LUMO+4    | CT                                  |
|          |                  | S <sub>6</sub>  | 283.0          | 0.003  | HOMO-1 $\rightarrow$ LUMO    | CT                                  |
|          |                  | S <sub>7</sub>  | 277.1          | 0.10   | HOMO-1 $\rightarrow$ LUMO+3  | LE                                  |
|          |                  | S <sub>8</sub>  | 275.8          | 0.0001 | HOMO $\rightarrow$ LUMO+5    | CT                                  |
|          |                  | S <sub>9</sub>  | 275.6          | 0.01   | HOMO-1 $\rightarrow$ LUMO+1  | CT                                  |
|          |                  | S <sub>10</sub> | 267.6          | 0.003  | HOMO $\rightarrow$ LUMO+6    | CT                                  |
| <b>2</b> | Default $\omega$ | S <sub>1</sub>  | 292.6          | 0.13   | HOMO $\rightarrow$ LUMO+1    | LE                                  |
|          |                  | S <sub>2</sub>  | 291.9          | 0.04   | HOMO $\rightarrow$ LUMO+2    | LE                                  |
|          |                  | S <sub>3</sub>  | 278.2          | 0.17   | HOMO $\rightarrow$ LUMO      | CT                                  |
|          |                  | S <sub>4</sub>  | 267.7          | 0.12   | HOMO $\rightarrow$ LUMO+3    | CT                                  |
|          |                  | S <sub>5</sub>  | 261.7          | 0.15   | HOMO-2 $\rightarrow$ LUMO+1  | LE                                  |
|          |                  | S <sub>6</sub>  | 261.0          | 0.55   | HOMO-2 $\rightarrow$ LUMO+2  | LE                                  |
|          |                  | S <sub>7</sub>  | 260.2          | 0.27   | HOMO-1 $\rightarrow$ LUMO+3  | LE                                  |
|          |                  | S <sub>8</sub>  | 252.5          | 0.07   | HOMO-1 $\rightarrow$ LUMO    | CT                                  |
|          |                  | S <sub>9</sub>  | 240.5          | 0.07   | HOMO-1 $\rightarrow$ LUMO+16 | LE                                  |
|          |                  | S <sub>10</sub> | 238.3          | 0.63   | HOMO $\rightarrow$ LUMO+16   | LE + CT                             |
| <b>2</b> | $\omega$ -CPCM   | S <sub>1</sub>  | 338.7          | 0.016  | HOMO $\rightarrow$ LUMO      | CT                                  |
|          |                  | S <sub>2</sub>  | 333.4          | 0.003  | HOMO $\rightarrow$ LUMO+1    | CT                                  |
|          |                  | S <sub>3</sub>  | 327.3          | 0.003  | HOMO-1 $\rightarrow$ LUMO    | CT                                  |
|          |                  | S <sub>4</sub>  | 322.2          | 0.006  | HOMO-1 $\rightarrow$ LUMO+1  | CT                                  |
|          |                  | S <sub>5</sub>  | 312.2          | 0.073  | HOMO $\rightarrow$ LUMO+3    | LE                                  |
|          |                  | S <sub>6</sub>  | 311.4          | 0.019  | HOMO $\rightarrow$ LUMO+4    | LE                                  |
|          |                  | S <sub>7</sub>  | 296.2          | 0.010  | HOMO $\rightarrow$ LUMO+2    | CT                                  |
|          |                  | S <sub>8</sub>  | 293.9          | 0.001  | HOMO $\rightarrow$ LUMO+5    | CT                                  |
|          |                  | S <sub>9</sub>  | 291.3          | 0.001  | HOMO-2 $\rightarrow$ LUMO    | CT                                  |
|          |                  | S <sub>10</sub> | 290.9          | 0.001  | HOMO-3 $\rightarrow$ LUMO    | CT                                  |

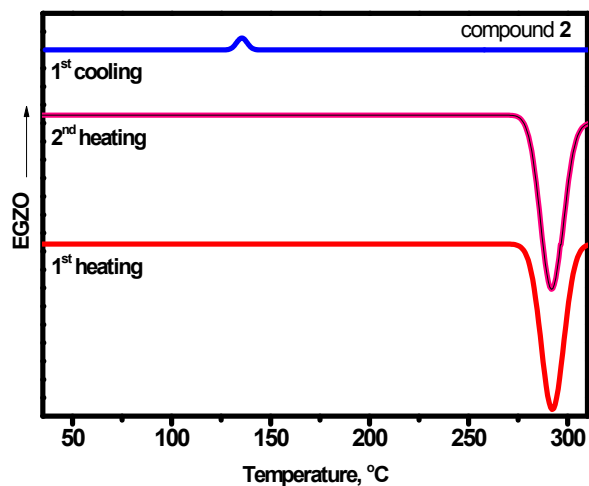
<sup>a</sup>Where CT = charge transfer state, LE = local excitation and LE + CT is a mix of these excitations



a)



b)



c)

**Figure S1.** DSC and TGA thermograms of compounds 1 and 2

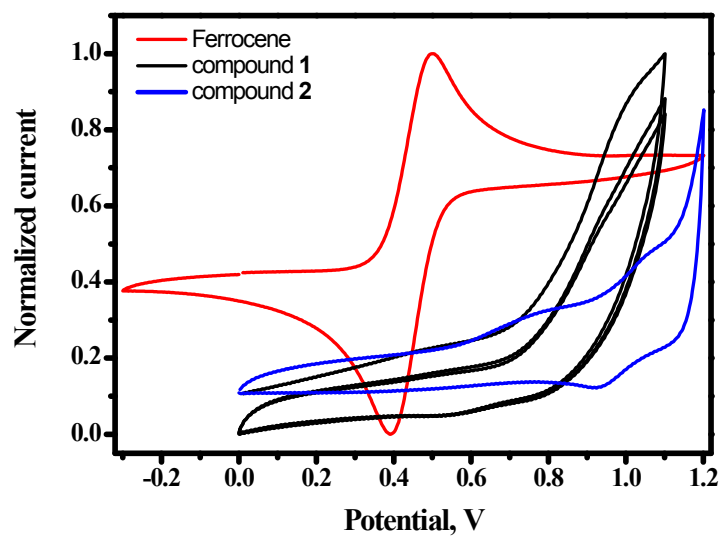


Figure S2. Cyclic voltammograms of solid samples of compounds 1 and 2.

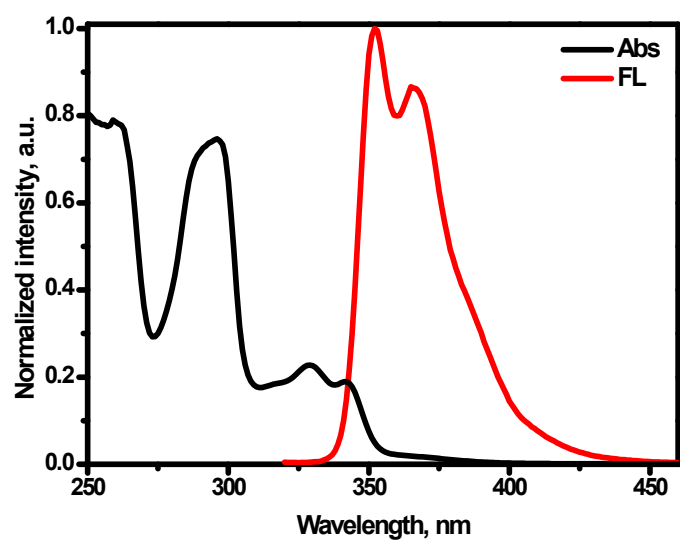
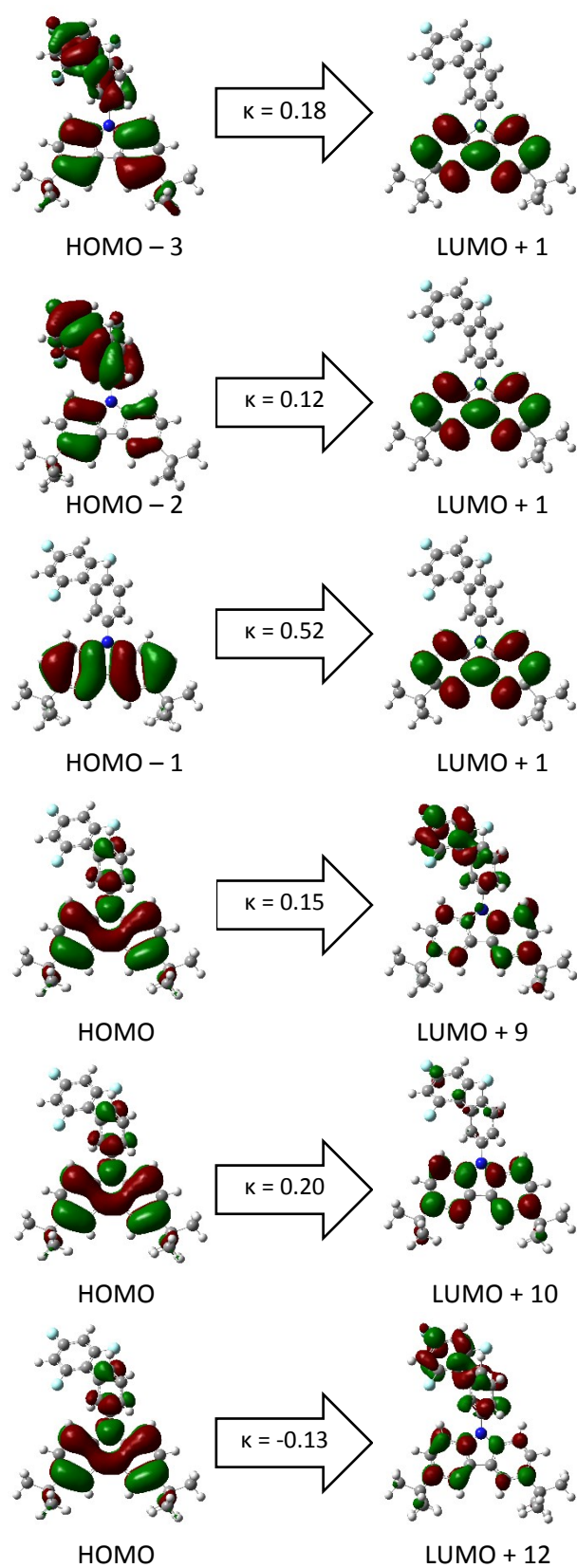
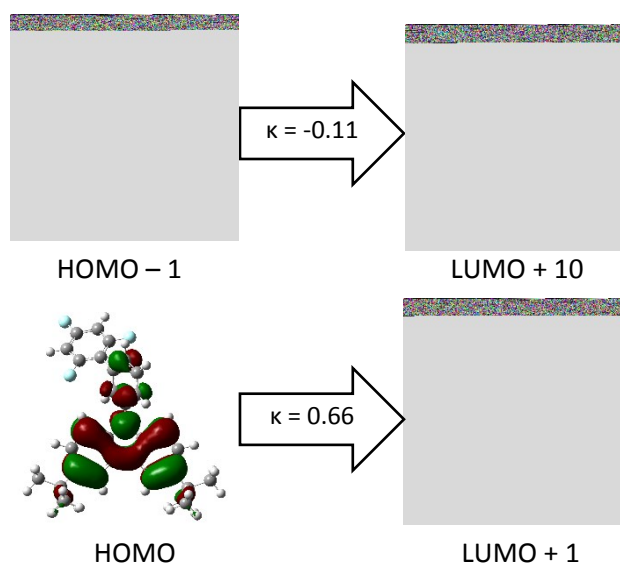


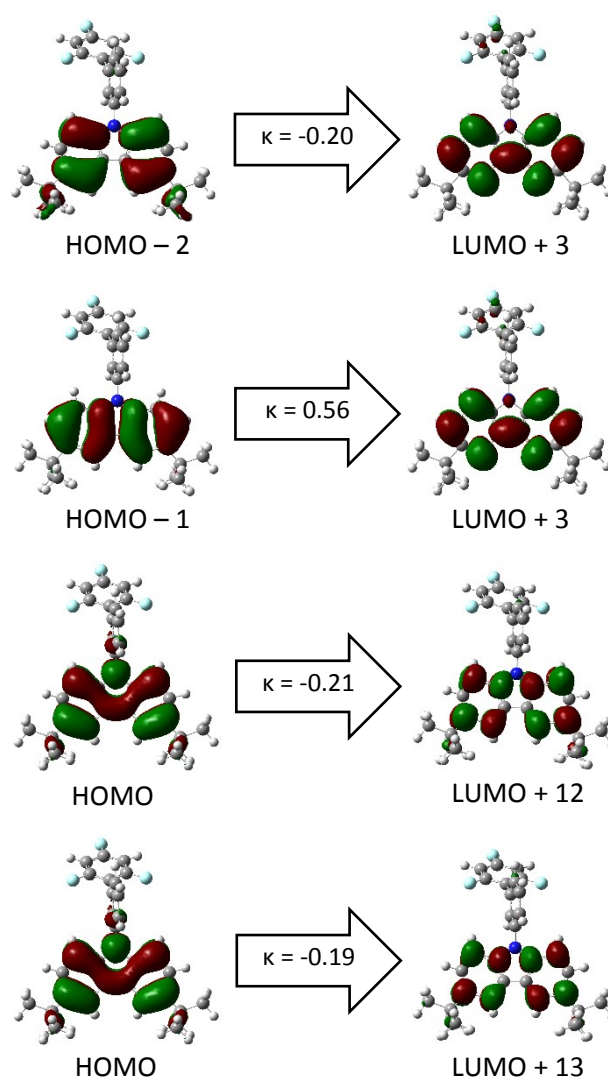
Figure S3. Absorption and fluorescence spectra of 9H-carbazole toluene solution



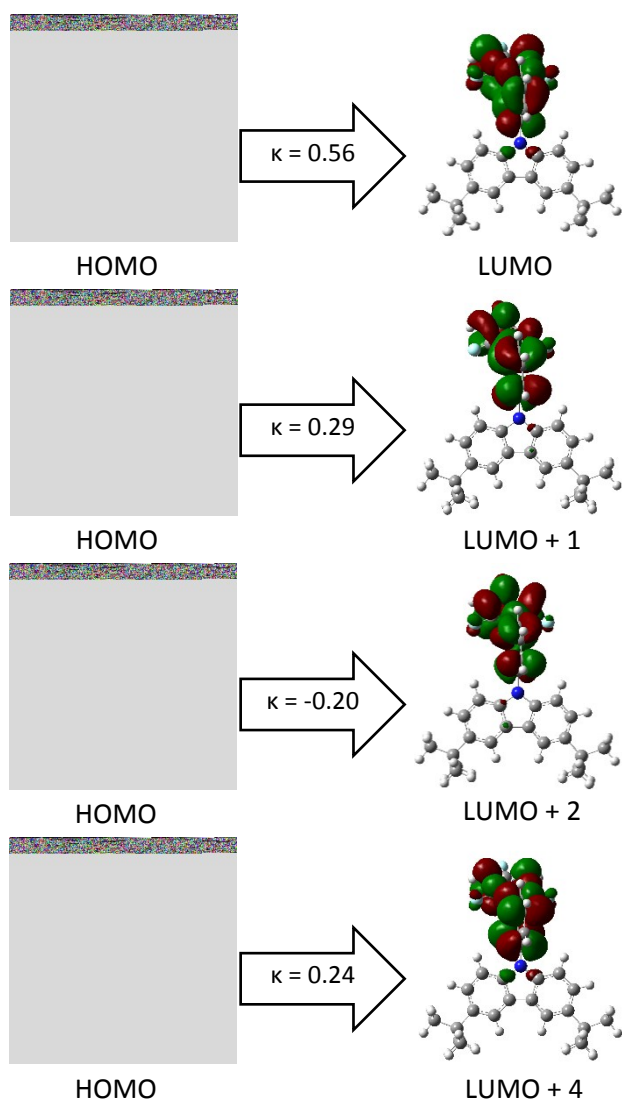
**Figure S4.** Transitions for  $T_1$  excitation of compound **1** determined by TDDFT.  $\omega$ B97XD/6-31++G(d,p), default  $\omega$



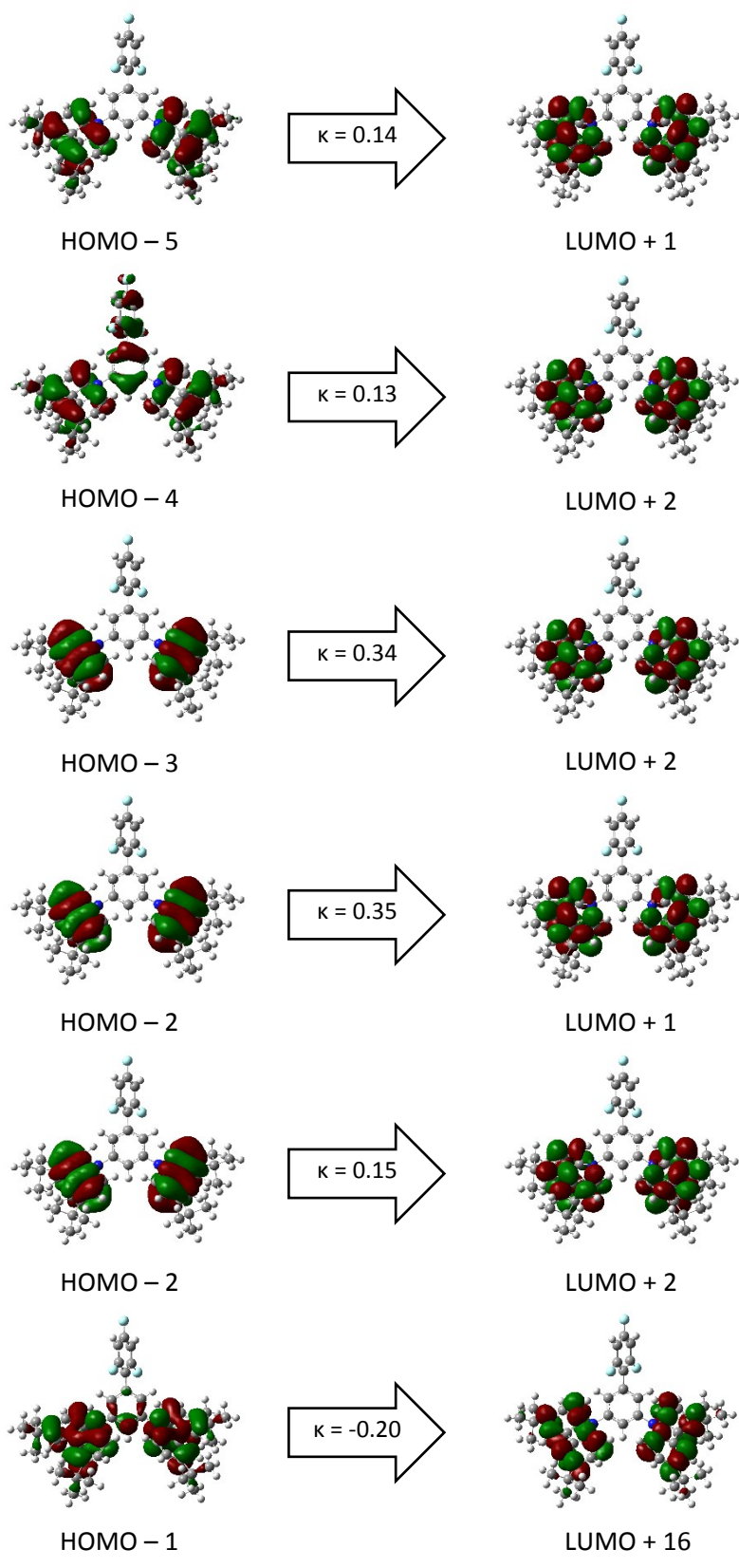
**Figure S5.** Transitions for  $S_1$  excitation of compound **1** determined by TDDFT.  $\omega$ B97XD/6-31++G(d,p), default  $\omega$



**Figure S6.** Transitions for  $T_1$  excitation of compound **1** determined by TDDFT.  $\omega$ B97XD/6-31++G(d,p),  $\omega$ -CPCM



**Figure S7.** Transitions for S<sub>1</sub> excitation of compound **1** determined by TDDFT.  $\omega$ B97XD/6-31++G(d,p),  $\omega$ -CPCM



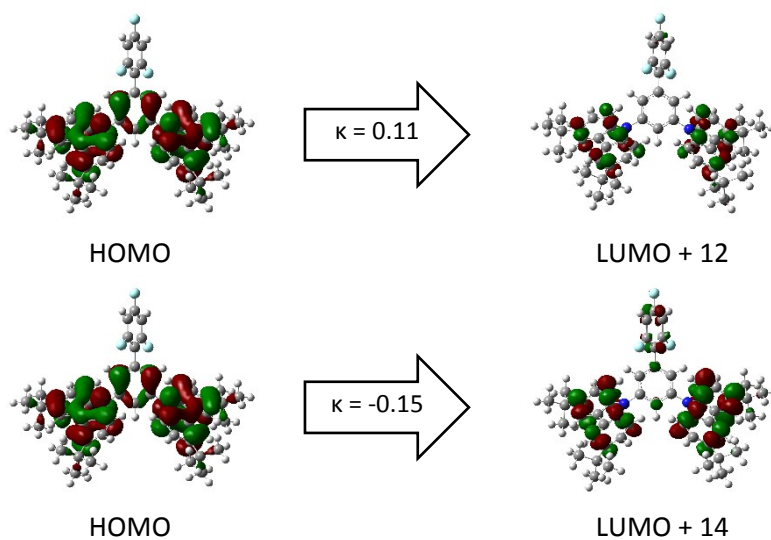


**Figure S8.** Transitions for  $T_1$  excitation of compound **2** determined by TDDFT.  $\omega$ B97XD/6-31++G(d,p), default  $\omega$

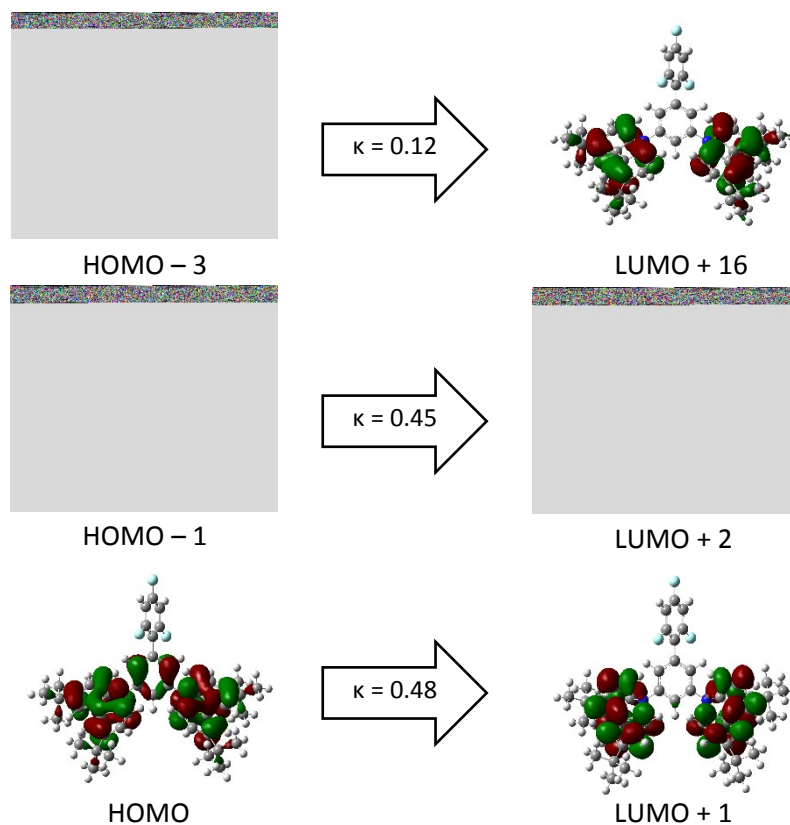
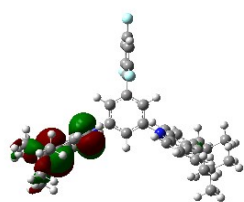
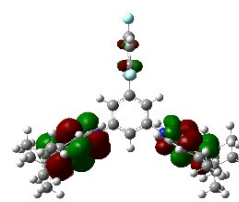
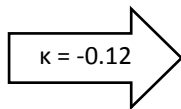


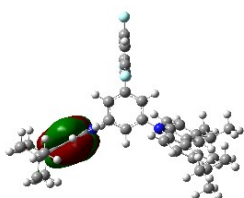
**Figure S9.** Transitions for  $S_1$  excitation of compound **2** determined by TDDFT.  $\omega$ B97XD/6-31++G(d,p), default  $\omega$



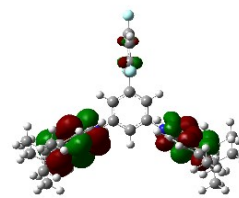
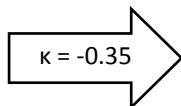
HOMO - 5



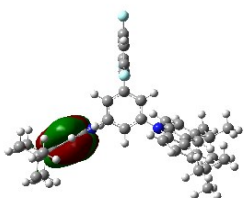
LUMO + 3



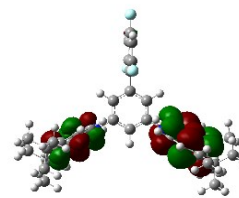
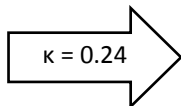
HOMO - 3



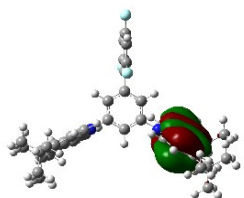
LUMO + 3



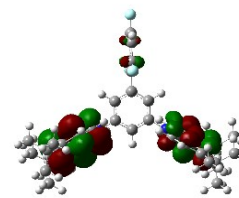
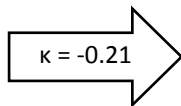
HOMO - 3



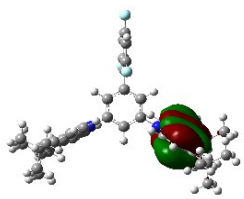
LUMO + 4



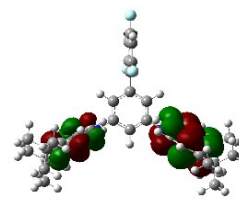
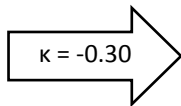
HOMO - 2



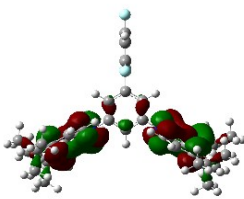
LUMO + 3



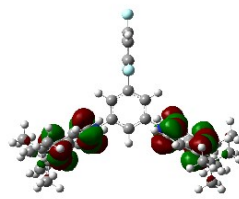
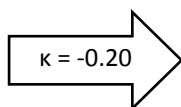
HOMO - 2



LUMO + 4



HOMO - 1



LUMO + 17

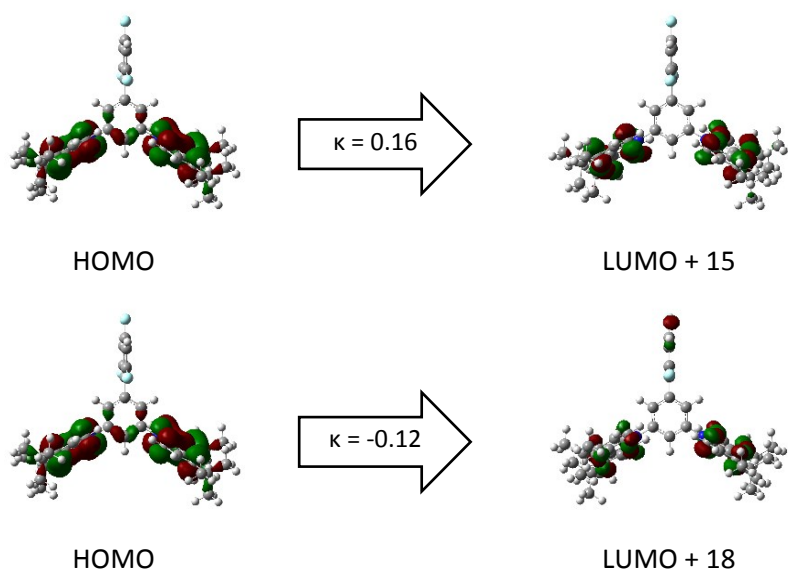


**Figure S10.** Transitions for  $T_1$  excitation of compound **2** determined by TDDFT.  $\omega$ B97XD/6-31++G(d,p),  $\omega$ -CPCM

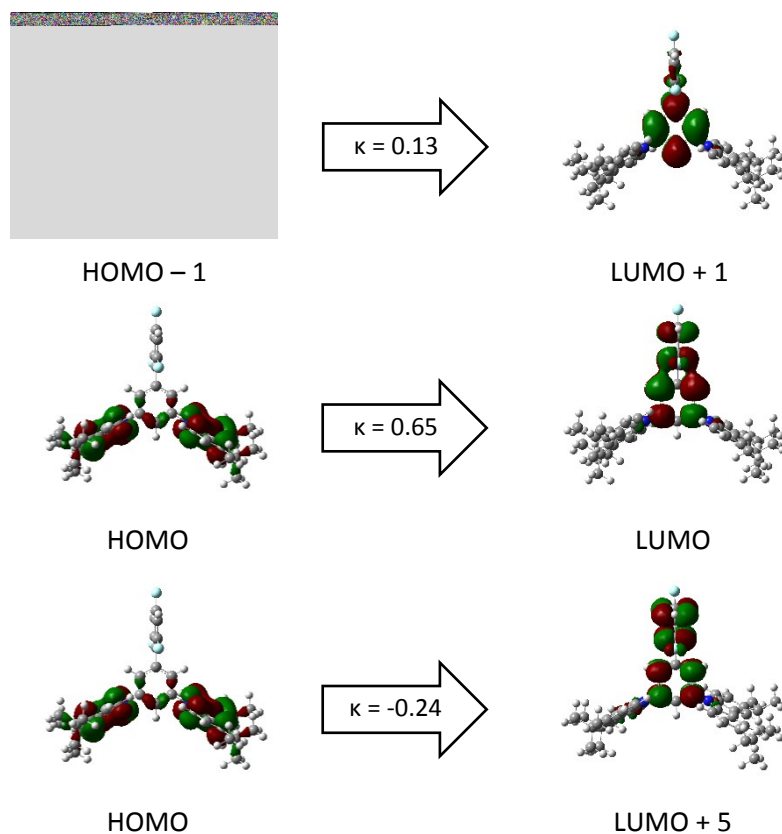


**Figure S11.** Transitions for  $S_1$  excitation of compound **2** determined by TDDFT.  $\omega$ B97XD/6-31++G(d,p),  $\omega$ -CPCM

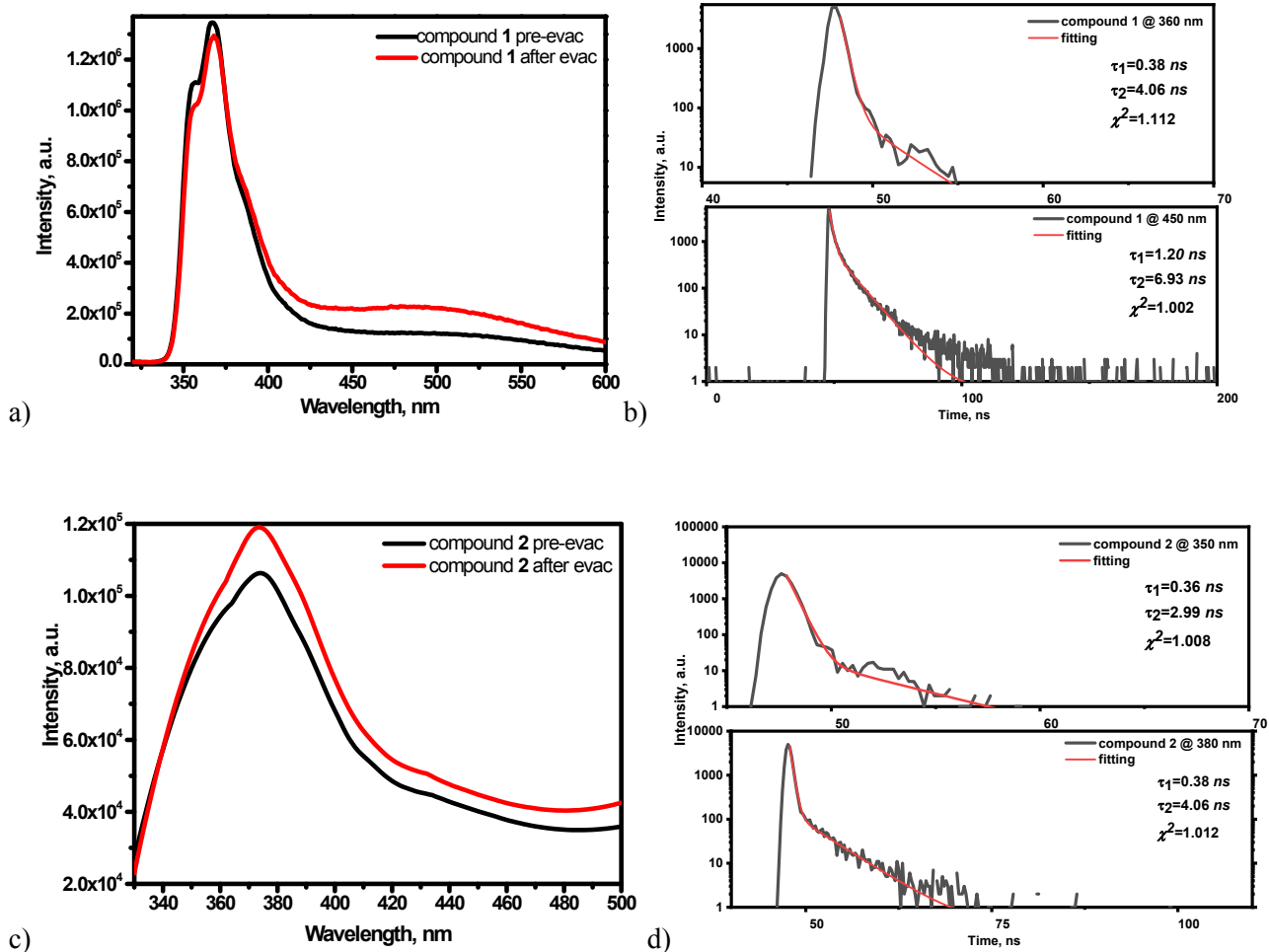


**Figure S12.** Fluorescence spectra (a) and PL decays (b) of solid films of carbazole-substituted compounds 1 and 2 under air and deoxygenated conditions.

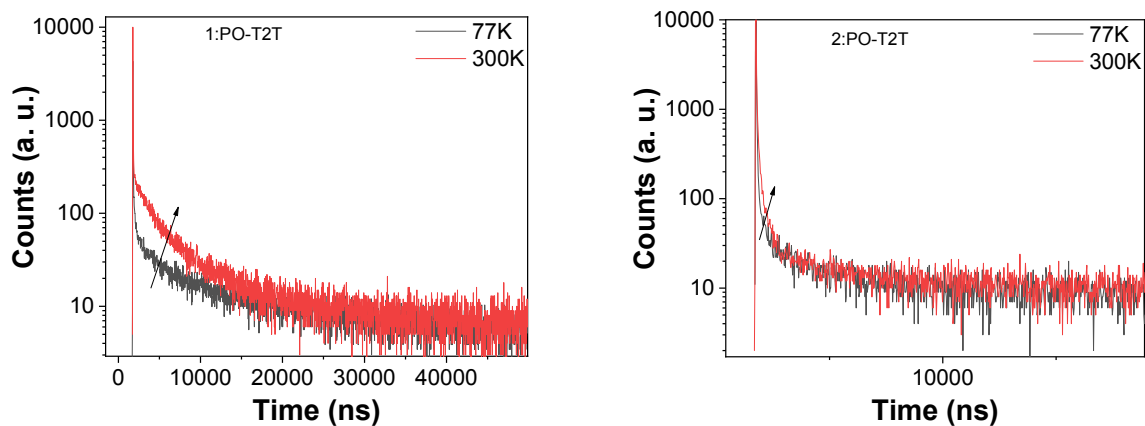


**Figure S13.** PL decays of molecular mixtures 1: PO-T2T and 2: PO-T2T at 295 and 77K.

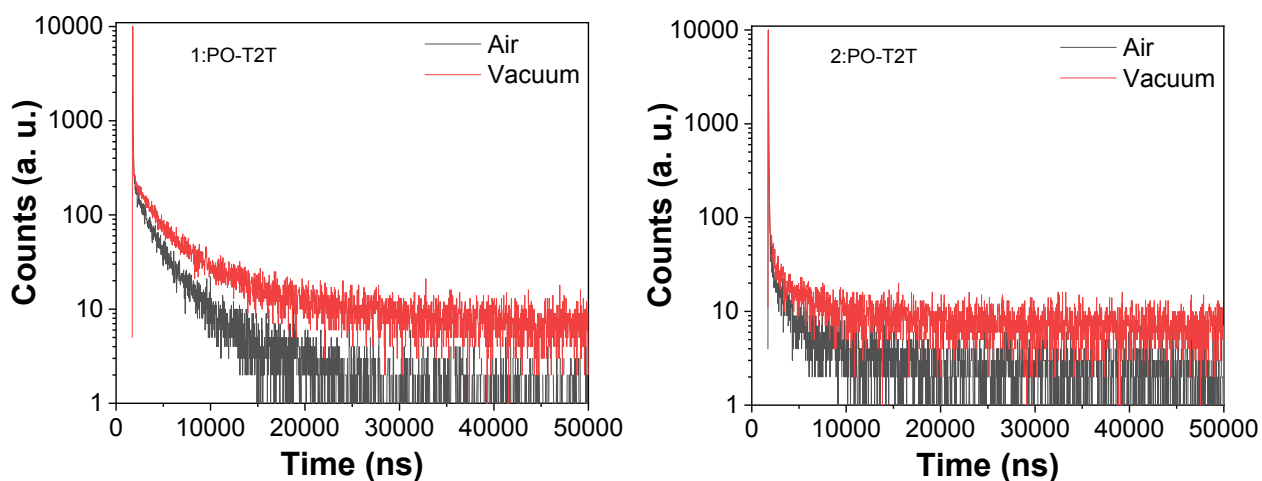


Figure S14. PL decays of molecular mixtures 1: PO-T2T and 2: PO-T2T under air and vacuum conditions.

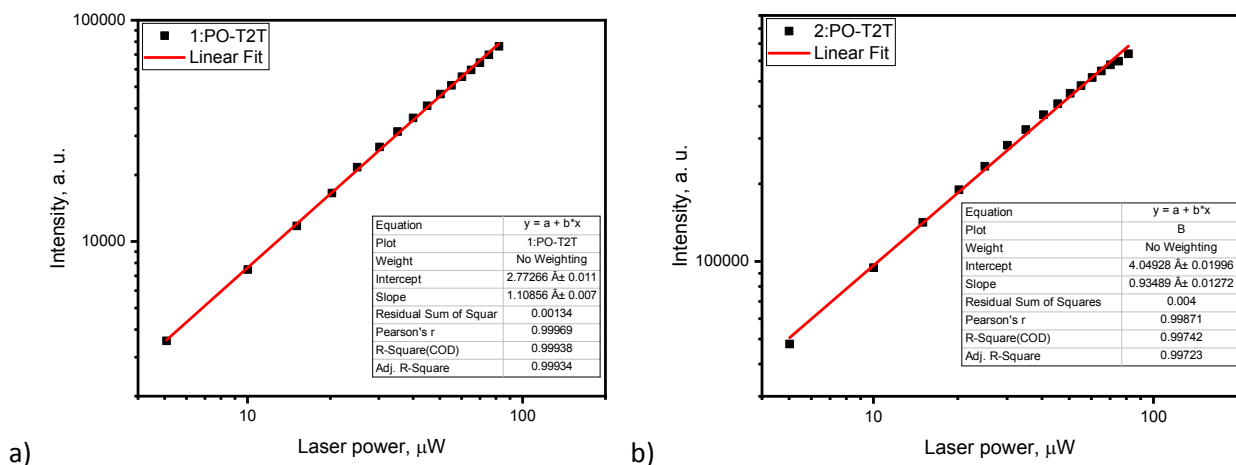


Figure S15. Fluorescence intensity dependence on laser pump pulse energy of solid samples of compound 1 and 2 at RT with delay of 800 ns.

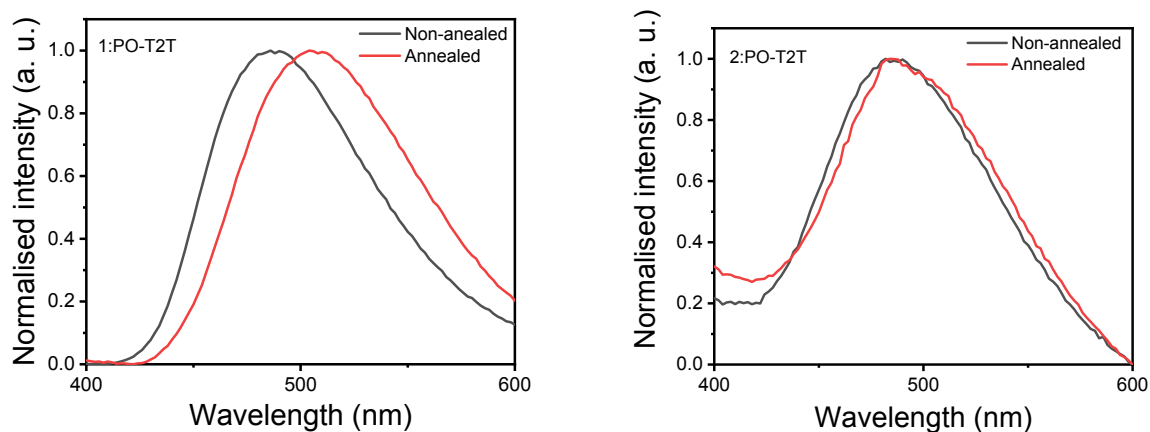
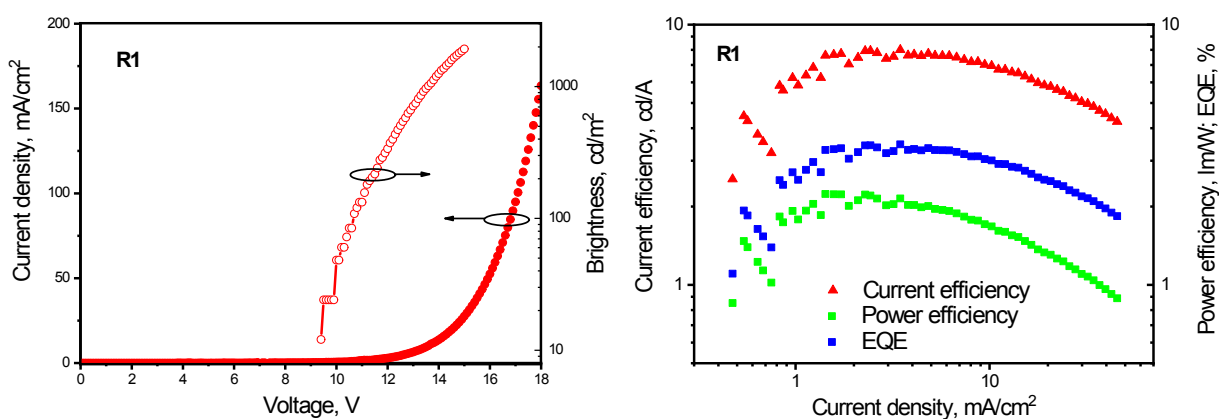
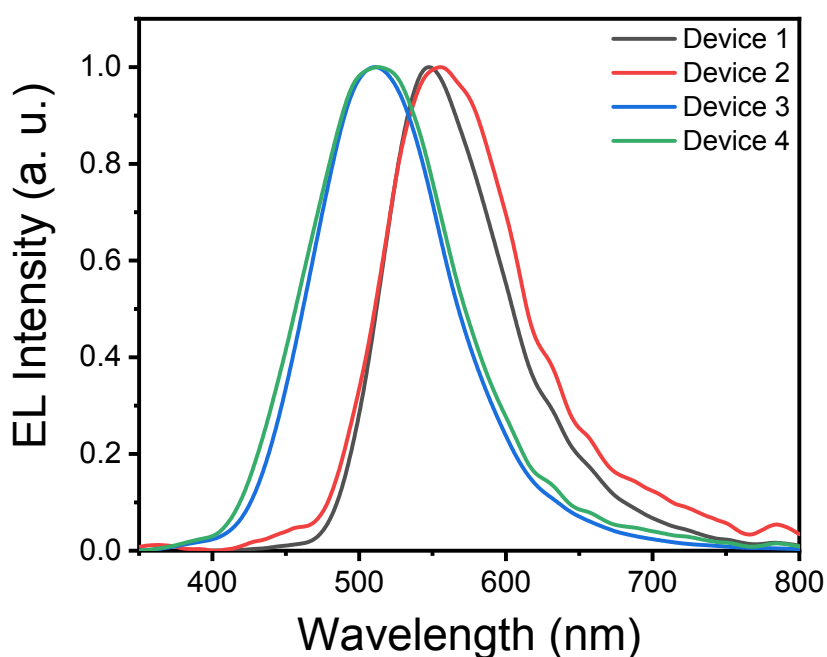


Figure S16. PL spectra of molecular mixtures 1: PO-T2T and 2: PO-T2T before and after thermal annealing.



**Figure S17.** a) Current density and brightness versus voltage plots, and b) EQEs, current and power efficiencies versus brightness plots for device R1.



**Figure S18.** EL spectra of devices  $\text{Mo}_2\text{O}_3$  / TAPC/ mCP/ compound 1:PO-T2T/TSP01/TPBi/LiF/Al (**Device 1**);  $\text{Mo}_2\text{O}_3$  / TAPC/ compound 1/ compound 1:PO-T2T/TSP01/TPBi/LiF/Al (**Device 2**);  $\text{Mo}_2\text{O}_3$  / TCTA/ mCP/ compound 1:PO-T2T/TSP01/TPBi/LiF/Al (**Device 3**);  $\text{Mo}_2\text{O}_3$  / TCTA/ compound 1/ compound 1:PO-T2T/TSP01/TPBi/LiF/Al (**Device 4**).

## References

- 1 Denshi Shashin Gakkai., *Denshi shashin = Electrophotography.*, Denshin Shashin Gakkai, 1959.
- 2 G. Gritzner and J. Kuta, *Pure and Applied Chemistry*, 1984, **56**, 461–466.
- 3 J. Da Chai and M. Head-Gordon, *Physical Chemistry Chemical Physics*, 2008, **10**, 6615–6620.
- 4 V. Barone and M. Cossi, *Journal of Physical Chemistry A*, 1998, **102**, 1995–2001.
- 5 H. Sun, S. Ryno, C. Zhong, M. K. Ravva, Z. Sun, T. Körzdörfer and J. L. Brédas, *Journal of Chemical Theory and Computation*, 2016, **12**, 2906–2916.
- 6 M. J. G. Peach, P. Benfield, T. Helgaker and D. J. Tozer, *Journal of Chemical Physics*, , DOI:10.1063/1.2831900.
- 7 M. J. Frisch, G. W. Trucks, H. B. Schlegel, G. E. Scuseria, M. A. Robb, J. R. Cheeseman, G. Scalmani, V. Barone, G. A. Petersson, H. Nakatsuji, X. Li, M. Caricato, A. V. Marenich, J. Bloino, B. G. Janesko, R. Gomperts, B. Mennucci, H. P. Hratchian, J. V. Ortiz, A. F. Izmaylov, J. L. Sonnenberg, D. Williams-Young, F. Ding, F. Lipparini, F. Egidi, J. Goings, B. Peng, A. Petrone, T. Henderson, D. Ranasinghe, V. G. Zakrzewski, J. Gao, N. Rega, G. Zheng, W. Liang, M. Hada, M. Ehara, K. Toyota, R. Fukuda, J. Hasegawa, M. Ishida, T. Nakajima, Y. Honda, O. Kitao, H. Nakai, T. Vreven, K. Throssell, J. A. Montgomery Jr., J. E. Peralta, F. Ogliaro, M. J. Bearpark, J. J. Heyd, E. N. Brothers, K. N. Kudin, V. N. Staroverov, T. A. Keith, R. Kobayashi, J. Normand, K. Raghavachari, A. P. Rendell, J. C. Burant, S. S. Iyengar, J. Tomasi, M. Cossi, J. M. Millam, M. Klene, C. Adamo, R. Cammi, J. W. Ochterski, R. L. Martin, K. Morokuma, O. Farkas, J. B. Foresman and D. J. Fox, 2009.
- 8 A. Kormos, I. Móczár, A. Sveiczter, P. Baranyai, L. Párkányi, K. Tóth and P. Huszthy, *Tetrahedron*, 2012, **68**, 7063–7069.
- 9 H.-Y. Chen, C.-T. Chen and C.-T. Chen, *Macromolecules*, 2010, **43**, 3613–3623.
- 10 W. Song, H. L. Lee and J. Y. Lee, *Journal of Materials Chemistry C*, 2017, **5**, 5923–5929.
- 11 B. Yadagiri, K. Narayanaswamy, R. Srinivasa Rao, A. Bagui, R. Datt, V. Gupta and S. P. Singh, *ACS Omega*, 2018, **3**, 13365–13373.